PHILOSOPHICAL TRANSACTIONS OF THE ROYAL SOCIETY A MATHEMATICAL, PHYSICAL & ENGINEERING SCIENCES

Self–similar numerical solutions of the porous–medium equation using moving mesh methods

C.J. Budd, G.J. Collins, W.Z. Huang and R.D. Russell

Phil. Trans. R. Soc. Lond. A 1999 **357**, 1047-1077
doi: 10.1098/rsta.1999.0364

THE ROYAL SOCIETY

Self-similar numerical solutions of the porous-medium equation using moving mesh methods

By C. J. Budd[1], G. J. Collins[2], W. Z. Huang[3] and R. D. Russell[4]

[1]*Department of Mathematics, University of Bath, Claverton Down, Bath BA2 7AY, UK*
[2]*School of Mathematics, University of Bristol, Bristol BS8 1TW, UK*
[3]*Department of Mathematics, 405 Snow Hall, University of Kansas, Lawrence, KS 66045, USA*
[4]*Mathematics and Computer Science, Simon Fraser University, Burnaby, BC, Canada V5A 1S6*

This paper examines a synthesis of adaptive mesh methods with the use of symmetry to study a partial differential equation. In particular, it considers methods which admit discrete self-similar solutions, examining the convergence of these to the true self-similar solution as well as their stability. Special attention is given to the nonlinear diffusion equation describing flow in a porous medium.

Keywords: porous-medium equation; self-similar solution; Lie-group invariance; conservation laws; mesh adaptation; equidistribution

1. Introduction

(*a*) *Preliminaries*

When analysing a parabolic partial differential equation (PDE) of the general form

$$u_t = f(x, u, u_x, u_{xx}) \tag{1.1}$$

we often seek changes of the dependent variable u and spatial variable x to new variables v, y such that a (locally invertible) transformation exists of the form

$$v \equiv v(t, x, u), \qquad y \equiv y(t, x, u). \tag{1.2}$$

If v and y are chosen appropriately, then often the equation (1.1) can be simplified, making the solution easier and emphasizing asymptotic effects. This process was systematized early in this century by Lie who observed that many of the celebrated PDEs of mathematical physics were invariant under the action of a symmetry group and that groupings of variables that were invariant under the action of the group made effective transformed variables. A description of this approach is given in Olver (1986). Solutions of the PDE which are themselves invariant under the action of the group are termed *similarity solutions* and when expressed in terms of the transformed variables often satisfy much simpler equations than the original PDE—for example, the similarity solution may simply be the solution of an *ordinary* differential equation (ODE). The importance of similarity solutions lies in their ease of calculation, the fact that they often act as attractors for the more general solutions of the PDE and

the universality of their occurrence in important physical problems. Reviews of the role played by similarity solutions in continuous problems are given in Dresner (1983), Bluman & Cole (1974), Barenblatt (1996) and on discrete problems in Dorodnitsyn (1993).

A good example is the linear heat equation

$$u_t = u_{xx} \tag{1.3}$$

invariant under the action of the scaling transformation

$$t \to \lambda^2 t, \quad x \to \lambda x, \quad u \to \lambda^\alpha u, \quad \lambda > 0.$$

Taking new coordinates,

$$u = t^{-1/2} v, \quad x = t^{1/2} y, \quad s = \log(t), \tag{1.4}$$

and substituting into (1.3) gives

$$v_s = L(v) \equiv \tfrac{1}{2} v + \tfrac{1}{2} y v_y + v_{yy}. \tag{1.5}$$

Equation (1.5) has a steady-state solution $\bar{v}(y)$ satisfying $L(\bar{v}) = 0$ given by

$$\bar{v}(y) = A \mathrm{e}^{-y^2/4}.$$

This corresponds to a time-evolving solution of (1.4). The corresponding analysis of the solution and of its stability is somewhat easier for the transformed equation than for the original.

This short discussion gives a strong hint that an appropriate numerical method for solving (1.3) is one which can itself be transformed into a discretization of (1.5). The purpose of this paper is to give an analysis of such schemes applied to the nonlinear diffusion equation. To introduce this, suppose that we discretize (1.3) by using a method of lines formulation with a time-varying mesh $X_i(t)$, for which $U_i(t)$ is an approximation to $u(X_i(t), t)$. Such a procedure is described, for example, in Huang *et al.* (1994). Following Huang *et al.* (1994), to allow for the effects of the motion of the mesh, we discretize (1.3) expressed in the Lagrangian form

$$\frac{\mathrm{d}u}{\mathrm{d}t} - \frac{\partial u}{\partial x}\frac{\mathrm{d}x}{\mathrm{d}t} = \frac{\partial^2 u}{\partial x^2}. \tag{1.6}$$

Provided that the mesh is sufficiently regular, a second-order accurate discretization of this equation is then given by

$$\dot{U}_i - \left(\frac{U_{i+1} - U_{i-1}}{X_{i+1} - X_{i-1}}\right)\dot{X}_i = \frac{\left(\dfrac{U_{i+1} - U_i}{X_{i+1} - X_i}\right) - \left(\dfrac{U_i - U_{i-1}}{X_i - X_{i-1}}\right)}{\frac{1}{2}(X_{i+1} - X_{i-1})}, \tag{1.7}$$

where dots denote differentiation with respect to t. Now, suppose that the time-varying mesh is uniform with respect to i so that

$$X_{i+1}(t) - 2X_i(t) + X_{i-1}(t) = 0 \quad \text{or} \quad X_{i+1}(t) - X_i(t) = H(t). \tag{1.8}$$

The system (1.7), (1.8) then admits a discrete solution of the form

$$U_i(t) = t^{-1/2} V_i(s), \quad X_i(t) = t^{1/2} Y_i(s), \tag{1.9}$$

and on substituting into (1.7) we have (after some manipulation)

$$\dot{V}_i - \left(\frac{V_{i+1}-V_{i-1}}{Y_{i+1}-Y_{i-1}}\right)\dot{Y}_i = \tfrac{1}{2}V_i + \left(\frac{V_{i+1}-V_{i-1}}{Y_{i+1}-Y_{i-1}}\right)\tfrac{1}{2}Y_i + \frac{\left(\frac{V_{i+1}-V_i}{Y_{i+1}-Y_i}\right) - \left(\frac{V_i-V_{i-1}}{Y_i-Y_{i-1}}\right)}{\frac{1}{2}(Y_{i+1}-Y_{i-1})}, \tag{1.10}$$

where dots now denote differentiation with respect to s. The latter equation is precisely a second-order accurate discretization of the Lagrangian form of the transformed equation (1.5). Now, suppose that this latter equation has a steady-state solution $\bar{V}_i, \bar{Y}_i$. Such a steady state is a discretization of the steady-state solution $\bar{v}(y)$ of (1.5) on the (non-uniform) mesh given by $\bar{Y}_i$. The analysis of the time-dependent solutions of (1.7) then reduces to the analysis of the equilibrium solutions of (1.10), which is in principle a much simpler task. Thus $(\bar{V}_i, \bar{Y}_i)$ is a *discrete self-similar solution* of (1.10).

The essence of a dynamic adaptive method to solve an evolutionary problem is the inclusion of equations, in addition to (1.7), which specify the evolution of the mesh points X_i, and this process underlines most adaptive techniques for solving evolutionary problems. There are many possible ways of doing this, some of which are described in Huang *et al.* (1994), but a clear guideline is given by the above calculation. Namely, the mesh points should be allowed to evolve in such a manner that for the above problem the solution

$$X_i(t) = t^{1/2}Y_i$$

with Y_i constant should always be admitted as a possible solution of the equations describing the mesh evolution. Note that using a non-adaptive mesh with X_i constant automatically prevents this possibility. In this paper we explore methods of evolving the mesh that permit the possibility.

Traditionally, adaptive numerical methods have been hard to analyse because of the close coupling between the mesh and the solution. The solution $U_i(t)$ and the mesh $X_i(t)$ then become a large dynamical system which may, potentially, have complex dynamics unrelated to that of the underlying PDE. However, if the adaptive mesh in some way reflects the underlying dynamics of the PDE, then there is the possibility that the dynamics of the coupled mesh–solution system can actually be simplified. We have already seen this with our example of the heat equation, where we have reduced the study of a dynamic problem to a static problem. The main purpose of this paper is to extend the above observation to show that if adaptive numerical methods are used to solve a class of problems, then very accurate long-time dynamics of the solution can be recovered. A secondary feature of PDEs governed by a symmetry group is the existence of various conservation laws, which play a major role in determining the evolution of the system. Again, in this paper we demonstrate that an effective adaptive method can also recover discrete analogues of the conservation laws—which cannot hold if a non-adaptive method is used.

To focus the study of these issues, we concentrate in this paper on the study of the behaviour of adaptive numerical methods to study the *porous-medium equation* (PME), which is a nonlinear diffusion equation of the form

$$u_t = (uu_x)_x = \tfrac{1}{2}(u^2)_{xx}, \quad \text{where } u \geqslant 0, \tag{1.11}$$

taking

$$u(x,t) = 0 \text{ if } |x| \text{ is sufficiently large.} \tag{1.12}$$

These equations have a rich dynamics (see Vasquez 1992) including group invariance, associated conservation laws and solutions with sharp interfaces. Indeed there are well-defined interface points $s_-(t)$ and $s_+(t)$ such that $u > 0$ iff $s_-(t) < x < s_+(t)$. We describe some of this dynamics in § 2. We aim to show that an adaptive scheme, designed to be invariant under the action of the symmetry group of the underlying equation, admits a discrete self-similar solution which approximates the underlying self-similar solution. Provided that the discrete system obeys a suitable conservation law, these solutions correctly capture the dynamics of the underlying PDE, allowing convergence results to be established. We demonstrate this by constructing a centred finite-difference approximation $U_i(t)$ to $u(x,t)$, which uses a moving mesh $X_i(t)$ with $0 \leqslant i \leqslant N+1$ such that $X_0(t)$ approximates $s_-(t)$ and X_{N+1} approximates $s_+(t)$. Then, as $N \to \infty$ and for large t, we show by formal asymptotic methods that

$$\max_i |U_i(t) - u(X_i,t)| \sim t^{-1/3}\left(C_1 \frac{\log(N+1)}{(N+1)^2} + \mathcal{O}(1/t^{1/3})\right), \tag{1.13}$$

$$\left[\frac{|X_{N+1}-X_0|}{N+1}\sum_{i=0}^{N+1}(U_i(t)-u(X_i,t))^2\right]^{1/2} \sim t^{-1/6}\left(C_2\frac{1}{(N+1)^2} + \mathcal{O}(1/t^{1/3})\right), \tag{1.14}$$

$$t^{-1/3}|X_0 - s_-(t)| = t^{-1/3}|X_{N+1} - s_+(t)| \sim C_3 \frac{\log(N+1)}{(N+1)^2} + \mathcal{O}(1/t^{1/3}). \tag{1.15}$$

Here C_1, C_2 and C_3 are constants which we estimate explicitly.

The layout of the remainder of this paper is as follows. In § 2 we briefly describe some of the dynamics of the porous-medium-equation problem and discuss the role played by conservation laws and similarity solutions. In § 3 we describe an adaptive method for solving (1.11) based upon equidistribution of the mesh points. In this derivation we consider the effect of conservation laws and the existence of self-similar solutions. We show that enforcing conservation leads to a scheme which has the correct asymptotics for large times but which gives suboptimal convergence as the mesh is refined. Our discussion will be illustrated by an exact solution. In § 4 we show how the equations so derived can be transformed so that they have a discrete self-similar solution as a steady state. In § 5 we construct such a solution and discuss the (suboptimal) convergence of this to the true self-similar solution as the number N of mesh points is refined. In § 6 we look at the stability as $t \to \infty$ of this solution, showing that it determines (correctly) the long-time dynamics of the underlying discrete system. In § 7 we combine these results to obtain the convergence estimates (1.13)–(1.15). Finally, in § 8 we present some numerical results which support our theoretical derivations.

2. The porous-medium equation and self-similar solutions

(a) *Existence*

The PME (1.11) arises in the study of the diffusion of gas through a porous medium under the action of the Darcy law relating velocity to pressure gradient (Dresner 1983). It also arises as a model of the swarming of various insect species (Murray 1989). More of the many applications and a summary of the analytic properties are given in Vasquez (1992). For this discussion we concentrate on three qualitative

features: solutions with compact support, conservation laws and scaling laws and associated self-similar solutions. There is now a fairly complete existence theory for the solutions of (1.11) based upon the application of semigroup theory and of the maximum principle. In particular, suppose that

$$u(0,x) \equiv u_0(x) \geqslant 0$$

and that $u_0(x) \in L_1(R)$ and has *compact* support. Then a global (weak) solution $u(x,t) \geqslant 0$ of (1.11) exists for all $t \geqslant 0$ which also has compact support. If the support is the set $S(t)$ and if $t_1 < t_2$, then

$$S(t_1) \subset S(t_2). \tag{2.1}$$

In the simplest case, $S(0)$ is an interval, and then $S(t)$ is an interval for all $t > 0$, and $u(x,t)$ has an interface at the two points $s_-(t) < s_+(t)$ such that $u(s_-,t) = u(s_+,t) = 0$, $u(x,t) = 0$ if $x \leqslant s_-$ or $x \geqslant s_+$ and $u(x,t)$ is non-zero in a right neighbourhood of s_- or a left neighbourhood of s_+. The interfaces propagate with a *finite* speed given by

$$\frac{\mathrm{d}s_\pm}{\mathrm{d}t} = -u(s_\pm,t)_x. \tag{2.2}$$

The regularity of the function $u(x,t)$ has been studied in some detail, and it is known that, under the above conditions, u is Lipschitz in a neighbourhood of the interface.

(*b*) *Conservation laws*

Two important conserved quantities of the solution are its integral and centre of mass. Suppose that a solution exists and

$$I(t) = \int_{-\infty}^{\infty} u\,\mathrm{d}x > 0. \tag{2.3}$$

Then

$$\frac{\mathrm{d}I}{\mathrm{d}t} = \int_{-\infty}^{\infty} u_t\,\mathrm{d}x = \int_{-\infty}^{\infty} (uu_x)_x\,\mathrm{d}x = 0.$$

Thus I is a constant. Similarly, if $\bar{x}$ is the scaled centre of mass

$$\bar{x} = \int_{-\infty}^{\infty} xu\,\mathrm{d}x, \tag{2.4}$$

then

$$\frac{\mathrm{d}\bar{x}}{\mathrm{d}t} = \int_{-\infty}^{\infty} xu_t\,\mathrm{d}x = \int_{-\infty}^{\infty} x(uu_x)_x\,\mathrm{d}y = -\int_{-\infty}^{\infty} uu_x\,\mathrm{d}x = -\frac{1}{2}\int_{-\infty}^{\infty} (u^2)_x\,\mathrm{d}x = 0.$$

Thus $\bar{x}$ is also a constant. We shall see in § 3 that both of these functions are also conserved with an appropriate adaptive numerical scheme.

(*c*) *Scaling laws and self-similar solutions*

Suppose now that we introduce a map from the original system (u,x,t) to a new system $(\hat{u},\hat{x},\hat{t})$ given by the (group) transformation

$$\hat{u} = \lambda^\alpha u, \quad \hat{x} = \lambda^\beta x, \quad \hat{t} = \lambda t, \tag{2.5}$$

where the constant λ is arbitrary; then we may rewrite (1.11) as a differential equation in $(\hat{u}, \hat{x}, \hat{t})$. Significantly, the equation in the new coordinates is identical to the original provided that

$$\alpha - 2\beta + 1 = 0. \tag{2.6}$$

The original system is then *scaling invariant* and (2.5) is a *scaling (or affine) transformation*. The set of all such transformations as λ varies over $(0, \infty)$ has a group structure. Suppose further that a solution of (1.11) exists which is itself invariant under these transformations so that

$$\lambda^{\alpha} u(x,t) = u(\lambda^{\beta} x, \lambda t). \tag{2.7}$$

Such a solution is an example of a *self-similar solution* of the form described in § 1. To find such a solution we seek coordinates that are invariant under the action of the transformation (2.5). Such coordinates are given by y and $v(y)$, where

$$y = x/t^{\beta}, \qquad v(y) = t^{-\alpha} u, \tag{2.8}$$

so that

$$u(x,t) = t^{\alpha} v(x/t^{\beta}). \tag{2.9}$$

From (2.3),

$$I = \int_{-\infty}^{\infty} u(x,t)\,\mathrm{d}x = t^{\alpha} \int_{-\infty}^{\infty} v(x/t^{\beta})\,\mathrm{d}x = t^{\alpha+\beta} \int_{-\infty}^{\infty} v(y)\,\mathrm{d}y.$$

As I is constant we deduce that

$$\alpha + \beta = 0, \qquad \beta = \tfrac{1}{3}. \tag{2.10}$$

Observe that this conservation law crucially determines the long-term dynamics of the solution. Substituting the expression (2.8) into the original PDE gives

$$0 = \tfrac{1}{3} v + \tfrac{1}{3} y v_y + (v v_y)_y. \tag{2.11}$$

Integrating (2.11) and applying the boundary conditions we have that v satisfies the *conservation law*

$$0 = \tfrac{1}{3} y v_y + (\tfrac{1}{2} v^2)_y. \tag{2.12}$$

This equation has a one-parameter family of solutions such that if $v(y)$ is a solution, then so is

$$\lambda^{-2} v(\lambda y), \tag{2.13}$$

where λ is arbitrary. The differential equation (2.12) was solved independently by Baranblatt and Pattle (Dresner 1983) to give the one-parameter family of solutions

$$v(y) = (a - \tfrac{1}{6} y^2)_+, \tag{2.14}$$

where a is a constant given by specifying the value of I and $v(y)$ has support $[-L, L]$ with

$$L = \sqrt{6a}.$$

A simple calculation gives

$$a^3 = \tfrac{3}{32} I^2 \quad \text{and} \quad L^3 = \tfrac{9}{2} I. \tag{2.15}$$

As the choice of the origin for both time t and space x was arbitrary, corresponding to (2.14) we have the family of self-similar solutions of (1.10) for general t_0 and x_0:

$$\bar{u}(x,t,a,x_0,t_0) = (t-t_0)^{-1/3}\left(a - \frac{(x-x_0)^2}{6(t-t_0)^{2/3}}\right)_+. \tag{2.16}$$

More generally, set

$$u(x,t) = t^{-1/3}v(x/t^{1/3},s) \quad \text{where } s = \log(t). \tag{2.17}$$

Substituting for $v(y,s)$ then gives

$$v_s = \tfrac{1}{3}v + \tfrac{1}{3}yv_y + (vv_y)_y \equiv (\tfrac{1}{3}yv + (\tfrac{1}{2}v^2)_y)_y, \tag{2.18}$$

which has the self-similar solution (2.14) as a steady state. Observe that

$$\int_{-\infty}^{\infty} v\,\mathrm{d}y \tag{2.19}$$

is a constant of the evolution. The self-similar solutions would be of academic interest only were it not for the following convergence result.

Theorem 2.1. *Let $u(x,t) \geqslant 0$ be an arbitrary solution of (2.18) with integral I and centre of mass x_0. Then if $\bar{u}(x,t;a,x_0,t_0)$ is the self-similar solution with the same integral and centre of mass, then for all t_0 we have*

$$t^{1/3}\|u-\bar{u}\|_{L_1} \to 0 \quad \text{as } t \to \infty. \tag{2.20}$$

Equivalently, the PDE (2.18) has as a global attractor the solution of the ODE (2.11) with the same first integral.

Proof. Proofs of this result use either the maximum principle or Lyapunov functions and are given in Kamenomostskaya (1973), Vasquez (1992) and Ralston (1984). ■

3. Moving mesh discretizations and associated conservation laws

(*a*) *The underlying scheme*

A good adaptive numerical method for solving the PME is one which can deal with arbitrary (positive) initial data but which has the correct asymptotic behaviour over long time-scales. This can be achieved at the cost of using a method which uses a first-order approximation for the boundary terms and which has a suboptimal convergence rate. To derive the method, we assume that $u(x,t)$ is approximated by $U_i(t)$ at the point $X_i(t)$, where U_i and X_i are chosen to give a consistent discretization of (1.11) expressed in Lagrangian form so that

$$\frac{\mathrm{d}u}{\mathrm{d}t} - \frac{\partial u}{\partial x}\frac{\mathrm{d}x}{\mathrm{d}t} = (uu_x)_x. \tag{3.1}$$

For this calculation we assume that the support of $u(x,t)$ is the interval $(s_-(t), s_+(t))$, which itself needs to be determined as part of the solution. We exploit this by placing mesh points $X_i(t)$, $i = 0,\ldots,N+1$ only within this interval such that

$$s_-(t) \approx X_0(t) < X_1(t) < X_2(t) < \cdots < X_N(t) < X_{N+1}(t) \approx s_+(t) \tag{3.2}$$

and

$$U_0(t) = U_{N+1}(t) = 0, \quad \text{for all } t. \tag{3.3}$$

To develop the scheme, we use three principles: (i) the scaling invariance of the discrete equation; (ii) the existence of a discrete conservation law; and (iii) the regularity of the solution at the interface. Using a central difference discretization of (3.1) for points $1 \leqslant i \leqslant N$ interior to the interface gives

$$\dot{U}_i - \left(\frac{U_{i+1} - U_{i-1}}{X_{i+1} - X_{i-1}}\right)\dot{X}_i = \frac{2}{(X_{i+1} - X_{i-1})}\left(\tfrac{1}{2}(U_{i+1} + U_i)\left(\frac{U_{i+1} - U_i}{X_{i+1} - X_i}\right) - \tfrac{1}{2}(U_i + U_{i-1})\left(\frac{U_i - U_{i-1}}{X_i - X_{i-1}}\right)\right). \tag{3.4}$$

This system is invariant to the scaling action of the symmetry group given by

$$t \to \lambda t, \quad U_i \to \lambda^\alpha U_i, \quad X_i \to \lambda^\beta X_i, \quad \forall \alpha, \beta.$$

In this formulation, we have placed no condition upon the location or movement of the mesh points. A natural first step is to determine X_0 and X_{N+1} by discretizing the condition (2.2) on the speed of the interfaces. As a first approximation we use a first-order discretization to give

$$\dot{X}_0 = -\frac{U_1}{(X_1 - X_0)} \quad \text{and} \quad \dot{X}_{N+1} = \frac{U_N}{(X_{N+1} - X_N)}. \tag{3.5}$$

From a sufficiently regular mesh, this discretization is to a lower order than that for the function U_i and consequently has a larger truncation error. We use it as it allows a discrete conservation law.

(*b*) *Conservation laws*

(i) *Conservation of the first integral*

An important feature of the system (3.4), (3.5) is that it admits a discrete form of conservation of the first integral of the solution.

Theorem 3.1. *Suppose that I_N is a discrete first integral of u given by*

$$I_N = \sum_{i=0}^{N} \tfrac{1}{2}(U_i + U_{i+1})(X_{i+1} - X_i). \tag{3.6}$$

Then if U_i and X_i satisfy (3.4), (3.5), I_N is a constant of the evolution.

Proof. From (3.6) we have

$$\frac{\mathrm{d}I_N}{\mathrm{d}t} = \frac{1}{2}\sum_{i=0}^{N}(\dot{U}_i + \dot{U}_{i+1})(X_{i+1} - X_i) + (U_{i+1} + U_i)(\dot{X}_{i+1} - \dot{X}_i).$$

Now, (3.4) can be written in the form

$$\dot{U}_i(X_{i+1} - X_{i-1}) - \dot{X}_i(U_{i+1} - U_{i-1}) = (D_i - D_{i-1}), \tag{3.7}$$

where

$$D_i = (U_{i+1} + U_i)\left(\frac{U_{i+1} - U_i}{X_{i+1} - X_i}\right).$$

Thus,

$$\begin{aligned}\sum_{i=1}^{N} \dot{U}_i(X_{i+1} - X_{i-1}) - \dot{X}_i(U_{i+1} - U_{i-1}) &= (D_N - D_0)\\ &= \left((U_{N+1} + U_N)\frac{U_{N+1} - U_N}{X_{N+1} - X_N} - (U_1 + U_0)\frac{U_1 - U_0}{X_1 - X_0}\right)\\ &= -U_N\dot{X}_{N+1} + U_1\dot{X}_0\end{aligned}$$

using (3.3), (3.5). Thus

$$\sum_{i=1}^{N} \dot{U}_i(X_{i+1} - X_{i-1}) - \dot{X}_i(U_{i+1} - U_{i-1}) + U_N\dot{X}_{N+1} - U_1\dot{X}_0 = 0.$$

However, after some manipulation, the expression above is simply $2\,\mathrm{d}I_N/\mathrm{d}t$, proving the result. ■

Note how the conservation of the mass is given by the first-order accurate description of the movement of the interface nodes. As an alternative to this scheme we might consider a second-order accurate scheme for the boundary conditions. Specifically, suppose that we take the simplest case of a uniform mesh with $X_{i+1} - X_i = H$ and use the scheme

$$\dot{X}_0 = -\left(\frac{4U_1 - U_2}{2H}\right), \quad \dot{X}_{N+1} = \left(\frac{4U_N - U_{N-1}}{2H}\right).$$

Defining I_N as above, we have

$$\begin{aligned}\dot{I}_N &= \tfrac{1}{2}U_N\left(\dot{X}_{N+1} - \frac{U_N}{H}\right) - \tfrac{1}{2}U_1\left(\dot{X}_0 + \frac{U_1}{H}\right)\\ &= \frac{1}{4H}((2U_N - U_{N-1}) + (2U_1 - U_2)).\end{aligned}$$

If the solution is ultimately convex (a property satisfied by the similarity solution), then $2U_N - U_{N-1}$ and $2U_1 - U_2$ are positive, and hence I_N increases for large times. We conclude that we cannot have conservation of mass and a second-order accurate boundary condition in such a case.

As conservation of mass determines the long-time asymptotics of the solution, we consider this the more important term to keep correct. Hence we use a less accurate boundary condition than the interior condition.

(ii) *Conservation of the centre of mass*

For the discrete system we define the discrete centre of mass $\bar{X}_N$ by

$$\bar{X}_N = \sum_{i=0}^{N}(X_{i+1} - X_i)(X_iU_i + X_{i+1}U_{i+1}). \tag{3.8}$$

Provided that the mesh points satisfy

$$X_{i+1} - 2X_i + X_{i-1} = 0, \quad \forall i,$$

then a similar calculation gives

$$\frac{\mathrm{d}\bar{X}_N}{\mathrm{d}t} = 0. \tag{3.9}$$

(c) *Calculation of the mesh points*

Now consider the motion of the mesh points interior to the support. The guiding principle here is that the equations so derived should be invariant to scaling transformations. In Budd *et al.* (1996*a*,*b*) and Budd & Collins (1998), a procedure for doing this is derived for problems with singularities that have a scaling invariance. It was proposed that the points should be equidistributed with respect to a monitor function M which itself was scaling invariant. We follow this procedure in a simple way here. Owing to the gentle nature of the evolution of the solution of the PME and the result (3.9), we simply take $M = 1$, which gives

$$X_{i+1} - 2X_i + X_{i-1} = 0, \quad i = 1, \ldots, N,$$

which is invariant under scaling. Equivalently,

$$X_{i+1} - X_i = H(t) = (X_{N+1} - X_0)/(N+1). \tag{3.10}$$

Combining (3.4), (3.5) and (3.10) gives a system in which the unknowns are U_i for $i = 0, \ldots, N+1$, X_0 and X_{N+1}, which is of the form

$$\dot{U}_i - \left(\frac{U_{i+1} - U_{i-1}}{2H}\right)\dot{X}_i = \frac{1}{2}\left(\frac{U_{i+1}^2 - 2U_i^2 + U_{i-1}^2}{H^2}\right) \quad i = 1, \ldots, N, \tag{3.11}$$

$$U_0 = U_{N+1} = 0, \tag{3.12}$$

$$\dot{X}_0 = -U_1/H, \quad \dot{X}_{N+1} = U_N/H, \quad H = (X_{N+1} - X_0)/(N+1). \tag{3.13}$$

This system can be solved by using an ODE solution package such as DASSL (Petzold 1982). Our calculations use this, and we presume for the remainder of the analysis in this paper that the ODEs can be solved exactly. It is worth noting, however, that although very accurate, this package does not necessarily give a system which is invariant to scalings in time. This property can be achieved by using instead an ODE solver (such as the forward Euler method) in which the time-step Δt is determined by the solution. For example taking $\Delta t = U_{N/2}^{-3}$ will lead to a scaling invariant method.

(d) *The dynamics when $N = 2$*

By looking at an exact solution we now investigate some further elementary properties of this system.

Lemma 3.2. *If $N = 2$, and (without loss of generality) $I_2 = 1$ and $\bar{X}_2 = \gamma$, then there are constants K, C such that*

$$U_1 = \tfrac{1}{2}(t+C)^{-1/3} + K(t+C)^{-5/3}, \quad U_2 = \tfrac{1}{2}(t+C)^{-1/3} - K(t+C)^{-5/3}, \tag{3.14}$$

$$\left.\begin{aligned} H &= (t+C)^{1/3}, \\ X_1 &= \gamma - \tfrac{1}{2}(t+C)^{1/3} + K(t+C)^{-1}, \\ X_2 &= \gamma + \tfrac{1}{2}(t+C)^{1/3} + K(t+C)^{-1}. \end{aligned}\right\} \tag{3.15}$$

Proof. To derive this solution we use the conserved invariants

$$I_2 = H(U_1 + U_2) \equiv 1, \quad \bar{X}_2 = H(X_1U_1 + X_2U_2) \equiv \gamma.$$

Now,

$$\dot{X}_0 = -U_1/H, \quad \dot{X}_3 = U_2/H, \quad \dot{X}_3 = \dot{X}_0 + 3\dot{H}$$

so that

$$3H\dot{H} = U_1 + U_2 = 1/H.$$

Integrating this expression gives a constant C for which

$$H = (t + C)^{1/3}, \quad \text{implying that } U_1 + U_2 = (t + C)^{-1/3}.$$

Rearranging $\bar{X}_2 = \gamma$ gives

$$\begin{aligned}\gamma &= \tfrac{1}{2}H((X_1 + X_2)(U_1 + U_2) + (X_1 - X_2)(U_1 - U_2)) \\ &= \tfrac{1}{2}(X_1 + X_2) - \tfrac{1}{2}H^2(U_1 - U_2);\end{aligned}$$

moreover,

$$\frac{U_2 - U_1}{H} = \dot{X}_0 + \dot{X}_3 = \dot{X}_1 + \dot{X}_2.$$

Thus, if $a = X_1 + X_2$ we have

$$2\gamma = a + H^3\dot{a} = a + (t + C)\dot{a}$$

so that there is a constant K for which

$$a = 2\gamma + \frac{2K}{t + C} \quad \text{and hence } U_2 - U_1 = -2K(t + C)^{-5/3}.$$

Combining these results gives (3.14) and the values of K and C then follow from the initial conditions. The values for X_1 and X_2 come from calculating X_0 using the interface motion condition. ■

This solution has both features in common with, and significant differences from, the solution of the underlying PDE. For large t it is clear that for arbitrary initial data, H, U_1 and U_2 tend toward the discrete similarity solution

$$H = t^{1/3}, \quad U_1 = U_2 = \tfrac{1}{2}t^{-1/3}, \quad X_2 = -X_1 = \tfrac{1}{2}t^{1/3}.$$

Indeed, for large t,

$$\begin{pmatrix} t^{1/3}U_1 \\ t^{1/3}U_2 \\ t^{-1/3}H \\ t^{-1/3}X_1 \\ t^{-1/3}X_2 \end{pmatrix} = \begin{pmatrix} 1/2 \\ 1/2 \\ 1 \\ -1/2 \\ 1/2 \end{pmatrix} + \frac{\gamma}{t^{1/3}}\begin{pmatrix} 0 \\ 0 \\ 0 \\ 1 \\ 1 \end{pmatrix} - \frac{C}{3t}\begin{pmatrix} 1/2 \\ 1/2 \\ -1 \\ 1/2 \\ -1/2 \end{pmatrix} + \frac{K}{t^{4/3}}\begin{pmatrix} 1 \\ -1 \\ 0 \\ 1 \\ 1 \end{pmatrix} + \mathcal{O}(1/t^2). \tag{3.16}$$

The behaviour above generalizes to the case of general N and motivates the analysis in the next three sections. In contrast, if we reduce t toward the value $-C$, then unless $K = 0$ the values U_i become opposite in sign and tend to infinity in absolute magnitude. This behaviour is in marked contrast to that of the continuous case in which the function tends towards a delta function in the same limit.

4. The discrete self-similar solution

Motivated by the existence and the central role played by the self-similar solution of the continuous problem, we now consider a self-similar solution of the discrete problem given by (3.11)–(3.13). To construct equations for the discrete self-similar solution, put

$$V_i(s) = t^{-\alpha}U_i, \quad Y_i = t^{-\beta}X_i, \quad \Lambda = t^{-\beta}H, \quad s = \log(t), \tag{4.1}$$

where we expect that V_i and Y_i should tend to steady-state solutions, implying that

$$\alpha - 2\beta + 1 = 0.$$

Furthermore,

$$I_N = \sum_{i=0}^{N} HU_i = t^{\alpha+\beta}\sum_{i=0}^{N} \Lambda V_i. \tag{4.2}$$

Hence, as I_N is conserved,

$$\alpha + \beta = 0 \quad \text{so that} \quad \alpha = -\tfrac{1}{3}, \quad \beta = \tfrac{1}{3}.$$

Most significantly, the resulting scaling is identical to that obtained for the continuous case and hence the discrete self-similar solution has the dynamics of the underlying solution over long time-intervals. Observe further that if a higher-order discretization of the boundary condition was used then I_N would *not* be conserved and hence the long-time dynamics of the discrete solution would be incorrect in this case. Of course over a *fixed* time-scale the latter method would give (asymptotically in N) a more accurate solution.

Substituting into (3.11)–(3.13) we obtain

$$\dot{V}_i - \left(\frac{V_{i+1} - V_{i-1}}{2\Lambda}\right)\dot{Y}_i = \tfrac{1}{3}V_i + \frac{1}{3}\left(\frac{V_{i+1} - V_{i-1}}{2\Lambda}\right)Y_i + \frac{1}{2}\left(\frac{V_{i+1}^2 - 2V_i^2 + V_{i-1}^2}{\Lambda^2}\right), \tag{4.3}$$

together with the boundary conditions

$$V_0 = V_{N+1} = 0 \tag{4.4}$$

and

$$\dot{Y}_0 + \tfrac{1}{3}Y_0 = -V_1/\Lambda, \quad \dot{Y}_{N+1} + \tfrac{1}{3}Y_{N+1} = V_N/\Lambda. \tag{4.5}$$

Here, dots denote differentiation with respect to s. Observe that (4.3) is a rescaling of (3.11), which is a discretization of (1.11). It is also precisely the equation that would be obtained by discretizing the rescaled equation (2.18). Thus the diagram in figure 1 commutes.

The system (4.3) has a steady-state solution satisfying

$$0 = \tfrac{1}{3}V_i + \frac{1}{3}\left(\frac{V_{i+1} - V_{i-1}}{2\Lambda}\right)Y_i + \frac{1}{2}\left(\frac{V_{i+1}^2 - 2V_i^2 + V_{i-1}^2}{\Lambda^2}\right) \tag{4.6}$$

with

$$\tfrac{1}{3}Y_0 = -V_1/\Lambda, \quad \tfrac{1}{3}Y_{N+1} = V_N/\Lambda,$$

which is a consistent discretization of the ODE (2.11). Again we make the observation that *the rescaled form of the discrete equation is identical to the discretization of the*

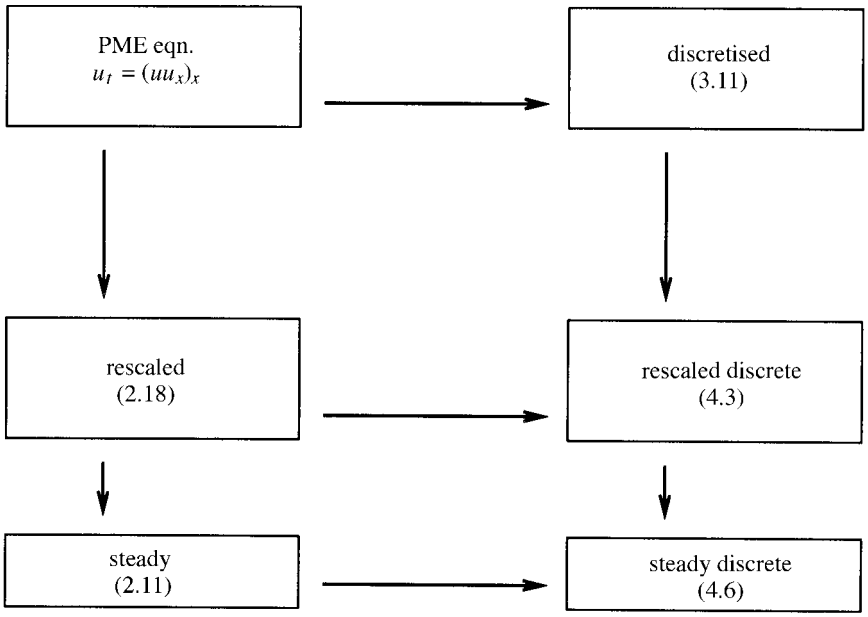

Figure 1. A commuting diagram showing the relation between the original, discrete and rescaled equations.

rescaled continuous equation. As in the continuous case, (4.6) has a one-parameter family of solutions such that if (V_i, Y_i) is a solution, then so is $(\lambda^2 V_i, \lambda Y_i)$ for arbitrary $\lambda > 0$. To fix the solution we impose the value of the discrete integral which, without loss of generality, we take to be one, so that

$$I_N \equiv \Lambda \sum_{i=0}^{N+1} V_i = 1. \tag{4.7}$$

The system (4.6) may be summed. To do this, set

$$\alpha_i = \frac{1}{6\Lambda}(V_{i+1}Y_i + V_iY_{i+1}) \quad \text{and} \quad \beta_i = \frac{1}{2\Lambda^2}(V_{i+1}^2 - V_i^2). \tag{4.8}$$

Then (4.6) reduces to

$$\alpha_i - \alpha_{i-1} + \beta_i - \beta_{i-1} = 0, \quad i = 1, \ldots, N. \tag{4.9}$$

Applying the boundary conditions at $i = 0$, $N+1$ and separating equations we then have

$$\alpha_i + \beta_i = 0, \quad i = 0, \ldots, N, \tag{4.10}$$

so that

$$\tfrac{1}{6}(V_{i+1}Y_i + V_iY_{i+1}) + \frac{1}{2\Lambda}(V_{i+1}^2 - V_i^2) = 0, \quad i = 0, \ldots, N, \tag{4.11}$$

which is a consistent discretization of (2.12). The numerical self-similar solution is given by the solution of (4.11) for $i = 0, \ldots, N$ together with the boundary conditions given in (4.4) and the condition (4.7). We note that the identity (4.11) automatically includes the boundary conditions (4.5). Numerical solutions of these equations can be found readily.

We now identify two key issues in our study of the system (4.3): (*i*) how well does the steady solution satisfying (4.11) converge to the solution of (2.12) as $N \to \infty$; and (*ii*) is such a steady state globally (or locally) stable? A combination of the answers to these two questions gives us insight into the convergence of the numerical algorithm, and we investigate them in the next two sections.

5. Convergence of the discrete self-similar solution as $N \to \infty$

We now investigate the convergence of the solution (V_i, Y_i) of the equations of the previous section to the true self-similar solution $v(y)$ as N increases. This calculation includes an estimate of the accuracy of the approximation to the support of the self-similar solution. Before we do this we observe that in order to obtain a scheme which conserves the first integral we had to use a lower-order approximation of the solution at the interface. As a consequence we observe a suboptimal convergence rate, and a full rigorous analysis of the convergence rate (based on the implicit function theorem) proves difficult. Instead we use an error-analysis technique based upon the method of matched asymptotic expansions. In this method two separate descriptions of the numerical solution are derived, one valid in a region which does not include the interface and a second valid in a region which does include the interface. These two solutions are then matched in a region for which both are valid.

To calculate the discrete self-similar solution we have determined both the point values V_i and the mesh points Y_i. To compare such a discrete self-similar solution V_i with the true self-similar solution $v(y)$, we presume that $I_N = 1$ and $I = 1$, so that $v(y) = (a - \frac{1}{6}y^2)$ if $-L \leqslant y \leqslant L$ with

$$L = \sqrt{6a} = (\tfrac{9}{2})^{1/3}, \quad a = (\tfrac{3}{32})^{1/3}$$

from (2.15). Now set

$$\lambda = 2L/(N+1), \quad v_i = v(-L + i\lambda), \quad \text{and} \quad y_i = -L + i\lambda$$

so that

$$y_i = -L + i\lambda = L\left(\frac{2i}{N+1} - 1\right) = \lambda(i - \tfrac{1}{2}(N+1)) \tag{5.1}$$

and

$$v_i = v(y_i) = \tfrac{1}{6}\lambda i(2L - i\lambda) = \frac{4a}{N+1} i\left(1 - \frac{i}{N+1}\right). \tag{5.2}$$

We can then compare V_i with v_i and Y_i with y_i and establish the following formal proposition.

Formal proposition 5.1. *If N is odd, then*

$$(i) \quad V_{(N+1)/2} - v_{(N+1)/2} \sim \frac{\alpha}{(N+1)^2}, \tag{5.3}$$

$$(ii) \quad \max_i (V_i - v_i) \sim \frac{2a\log(N+1)}{(N+1)^2}, \tag{5.4}$$

$$(iii) \quad Y_i \sim y_i\left(1 + \frac{\delta - \log(N+1)}{(N+1)^2}\right), \tag{5.5}$$

where

$$\alpha = 6^{1/3}(\tfrac{7}{6} - \log(2)) = 0.860\,442\ldots,$$
$$\delta = 6^{-2/3}(7 - \log(6)) + 2a(\log(a) - \gamma) = 0.336\,006\ldots$$

and γ is Euler's constant.

Observe that $V_i > v_i$ and $Y_{N+1} < L$.

Formal derivation. The discrete solution (V_i, Y_i, Λ) satisfies the conservation equation

$$\tfrac{1}{3}\Lambda(V_iY_{i+1} + V_{i+1}Y_i) + (V_{i+1}^2 - V_i^2) = 0. \tag{5.6}$$

Now set

$$V_i = v_i + w_i, \quad Y_i = y_i + z_i \quad \text{and} \quad \Lambda = \lambda + \mu,$$

where w_i, z_i and μ are all small, and let T be the truncation error defined by

$$T \equiv \tfrac{1}{3}\lambda(v_iy_{i+1} + v_{i+1}y_i) + (v_{i+1}^2 - v_i^2). \tag{5.7}$$

Linearizing (5.6) we have to leading order

$$T + \tfrac{1}{3}\mu(v_iy_{i+1} + v_{i+1}y_i) + 2(w_{i+1}v_{i+1} - w_iv_i) + \tfrac{1}{3}\lambda(v_iz_{i+1} + v_{i+1}z_i) + \tfrac{1}{3}\lambda(w_iy_{i+1} + w_{i+1}y_i) = 0. \tag{5.8}$$

Substituting the expressions for v_i and y_i into T gives

$$T = 16a^2(2i - N)/(N + 1)^4. \tag{5.9}$$

To analyse this system we apply the method of backward error analysis by considering the limit of $N \to \infty$ and $\lambda = 2\sqrt{6a}/(N + 1) \to 0$. In this limit the equation (5.7) is a consistent discretization of a differential equation satisfied by functions $w(y)$ and $z(y)$ which have point values w_i and z_i, with a truncation error that is asymptotically negligible as $N \to \infty$. By analysing the solutions of this equation we can then deduce the leading-order behaviour of w_i and z_i. Dividing by λ and setting

$$\mu/\lambda = \theta,$$

where θ is to be determined, we obtain in the limit

$$\frac{8a^2(2i - N)}{\sqrt{6a}(N + 1)^3} + \tfrac{2}{3}\theta vy + 2(wv)_y + \tfrac{2}{3}vz + \tfrac{2}{3}wy = 0. \tag{5.10}$$

Now, $y_i = \lambda(N + 1 - 2i)$ and $Y_i = \Lambda(N + 1 - 2i)$ so that

$$\frac{Y_i}{y_i} = 1 + \frac{z_i}{y_i} = \frac{\Lambda}{\lambda} = 1 + \frac{\mu}{\lambda} = 1 + \theta, \tag{5.11}$$

giving

$$z_i/y_i = \theta.$$

Moreover,

$$\frac{8a^2(2i - N)}{\sqrt{6a}(N + 1)^3} = \frac{8\sqrt{6a}a^2}{6a(N + 1)^2}\left(\frac{2i}{N + 1} - 1 + \frac{1}{N + 1}\right) = \frac{4ay}{3(N + 1)^2} + \mathcal{O}(1/(N + 1)^3).$$

Combining these results and considering leading-order terms only, we obtain

$$\tfrac{4}{3}\theta vy + 2(wv)_y + \tfrac{2}{3}wy = -\frac{4}{3}\frac{ay}{(N+1)^2}. \tag{5.12}$$

Now,

$$2(wv)_y + \tfrac{2}{3}wy = 2(w(a - \tfrac{1}{6}y^2))_y + \tfrac{2}{3}wy = 2w_y(a - \tfrac{1}{6}y^2) - \tfrac{2}{3}wy + \tfrac{2}{3}wy = 2vw_y,$$

so that

$$\tfrac{4}{3}\theta vy + 2vw_y = -\frac{4}{3}\frac{ay}{(N+1)^2}.$$

This equation has the exact solution

$$w = C - \tfrac{1}{3}\theta y^2 + \frac{2a}{(N+1)^2}\log(a - \tfrac{1}{6}y^2), \tag{5.13}$$

where C is a constant. Observe that $w(y)$ is singular as $y^2 \to 6a$. Hence, the expression (5.13) fails to be valid in this limit. Instead it is the outer solution of an expression which is valid close to the boundary. To determine the value of C compare the discrete sum to the integral of v. Thus

$$\begin{aligned}\Lambda\sum_{i=0}^{N+1} V_i = 1 &\Rightarrow (\lambda+\mu)\sum_{i=0}^{N+1}(v_i + w_i)\\ &= 1 \Rightarrow \left(\lambda\sum_{i=0}^{N+1} v_i - 1\right) + \lambda\sum_{i=0}^{N+1} w_i + \mu\sum_{i=0}^{N+1} v_i = 0.\end{aligned}$$

From the standard error analysis of the trapezium rule approximation we have that

$$\lambda\sum_{i=0}^{N+1} v_i - 1 = -\frac{1}{(N+1)^2}$$

and, to leading order in λ,

$$\lambda\sum_{i=0}^{N+1} w_i = \int_{-L}^{L} w\,\mathrm{d}y \quad \text{and} \quad \mu\sum_{i=0}^{N+1} v_i = \frac{\mu}{\lambda}\lambda\sum v_i = \theta\int_{-L}^{L} v\,\mathrm{d}y = \theta.$$

Hence, considering the limit of small λ we have

$$-\frac{1}{(N+1)^2} + \int_{-L}^{L} w\,\mathrm{d}y + \theta = 0.$$

Integrating the expression (5.13) and substituting for a gives

$$\int_{-L}^{L} w\,\mathrm{d}y = 2LC - \theta + \frac{2a}{(N+1)^2}\int_{-L}^{L}\log(a - \tfrac{1}{6}y^2)\,\mathrm{d}y.$$

Combining results gives

$$2LC = -\frac{2a}{(N+1)^2}\int_{-L}^{L}\log(a - \tfrac{1}{6}y^2)\,\mathrm{d}y + \frac{1}{(N+1)^2}.$$

Evaluating the integral and substituting the values of L, a we then have

$$C = \frac{6^{-2/3}(7 - \log(6))}{(N+1)^2} \equiv \frac{\kappa}{(N+1)^2} = \frac{1.577\,333\ldots}{(N+1)^2}.$$

Hence,

$$w(y) = -\tfrac{1}{3}\theta y^2 + \frac{\kappa}{(N+1)^2} + \frac{2a}{(N+1)^2}\log(a - \tfrac{1}{6}y^2). \tag{5.14}$$

Observe then that

$$(N+1)^2 w(0) = \kappa + 2a\log(a) = \alpha \equiv 6^{1/3}(\tfrac{7}{6} - \log(2)).$$

This is precisely the value taken by $V_i - v_i$ at $i = \frac{1}{2}(N+1)$, giving the result (5.3).

To complete the derivation of formal proposition 5.1 we determine the value of θ by looking at the contribution of the boundary terms. We concentrate on an analysis of the behaviour of w_i close to the left interface, fixing i and letting $N \to \infty$. To do this we now derive the following proposition.

Formal proposition 5.2. *In the limit of $N \to \infty$ we have*

$$w_{i+1} = w_i + \frac{4a}{(2i+1)(N+1)^2}. \tag{5.15}$$

Similar behaviour occurs close to the right interface.

Formal derivation. From the identity

$$\frac{16a^2(2i-N)}{(N+1)^4} + \tfrac{2}{3}\mu(v_i y_{i+1} + v_{i+1}y_i) + \tfrac{1}{3}\lambda(w_i y_{i+1} + w_{i+1}y_i) + 2(w_{i+1}v_{i+1} - w_i v_i) = 0, \tag{5.16}$$

and (5.1), (5.2); then if i is fixed and $N \to \infty$, we have

$$-\frac{16a^2}{(N+1)^3} - \tfrac{2}{3}\mu\sqrt{6a}\frac{4a}{(N+1)}(2i+1) - \tfrac{1}{3}\sqrt{6a}\lambda(w_i + w_{i+1}) + \frac{8a}{N+1}((i+1)w_{i+1} - i w_i) = 0. \tag{5.17}$$

Substituting for λ gives

$$\frac{16a^2}{(N+1)^2} = \tfrac{8}{3}\mu\sqrt{6a}(2i+1) + 4a((2i+1)w_{i+1} - (2i+1)w_i). \tag{5.18}$$

Now, $\mu/\lambda = \theta$ and we shall assume at present that

$$\theta = o(1/(N+1)) \quad \text{so that} \quad \mu = o(1/(N+1)^2)$$

(in fact we show presently that $\theta = \mathcal{O}(\log(N+1)/(N+1)^2)$. Making this assumption, the asymptotic contribution of the terms involving μ to (5.18) is zero and we have simply that

$$w_{i+1} = w_i + \frac{4a}{(2i+1)(N+1)^2}$$

as required. ■

This completes the derivation of formal proposition 5.2. Now we complete the derivation of formal proposition 5.1.

As $w_0 = 0$, if i is fixed, then in the limit of large N

$$\begin{aligned} w_i &= \frac{4a}{(N+1)^2}\left[1 + \tfrac{1}{3} + \cdots + \frac{1}{2i-1}\right] \\ &= \frac{4a}{(N+1)^2}[\tfrac{1}{2}\log(i) + \log(2) + \tfrac{1}{2}\gamma + \mathcal{O}(1/i^2)], \end{aligned} \tag{5.19}$$

where $\gamma = 0.577\,215\,664\,9015$ is Euler's constant.

Using (5.1) gives

$$i = \frac{(N+1)(y_i + L)}{2L},$$

and substituting gives

$$w_i = w(y_i) = \frac{2a}{(N+1)^2}(\log(y_i + L) + \log(N+1) - \log(2L)) + \frac{4a}{(N+1)^2}(\log(2) + \tfrac{1}{2}\gamma + \mathcal{O}(1/i^2)).$$

The limit of (5.14) as $y \to -L$ is then

$$w(y) \to -2a\theta + \frac{1}{(N+1)^2}[\kappa + 2a\log(2L) - 2a\log(6)] + \frac{2a}{(N+1)^2}\log(y+L).$$

If we now take i to be large but also have $y + L$ small (for example, if N is large, $i \sim \sqrt{N}$ and $y + L \sim 1/\sqrt{N}$), then these two expressions for $w(y)$ can be matched. Indeed, in this case they agree to order $1/(N+1)^3$ provided that

$$-2a\theta + \frac{1}{(N+1)^2}[\kappa + 2a\log(2L) - 2a\log(6)] = \frac{2a}{(N+1)^2}[\log(N+1) - \log(2L) + 2\log(2) + \gamma].$$

Evaluating the terms in this expression we then have

$$\theta = -\frac{\log(N+1)}{(N+1)^2} + \frac{\kappa + 2a(\log(a) - \gamma)}{(N+1)^2} = \frac{\delta - \log(N+1)}{(N+1)^2}, \tag{5.20}$$

where

$$\delta = \kappa + 2a(\log(a) - \gamma),$$

consistent with the earlier assumed bound on θ. This gives

$$w(y) = \frac{1}{3}\left(\frac{\log(N+1)}{(N+1)^2} - \frac{\delta}{(N+1)^2}\right)y^2 + \frac{\kappa}{(N+1)^2} + \frac{2a}{(N+1)^2}\log(a - \tfrac{1}{6}y^2). \tag{5.21}$$

This expression has a local minimum at $y = 0$ and a local maximum at

$$y = \pm\sqrt{6a\left(1 - \frac{1}{\log(N+1) - \delta}\right)}$$

at which points we have

$$\max(w) = \frac{1}{(N+1)^2}\left(2a(\log(N+1) - (1+\delta)) + \kappa + 2a\log\left(\frac{a}{\log(N+1) - \delta}\right)\right). \tag{5.22}$$

For very large N this is asymptotically

$$\max(w) = \frac{2a\log(N+1)}{(N+1)^2},$$

which gives (5.4). Finally, to show (5.5), the estimate for the error in the calculation of the grid, we use (5.11) and the estimate for θ. ■

6. The stability of the discrete self-similar solution as $t \to \infty$

We now look at the second question raised in § 4, namely the stability in time of the discrete self-similar solution.

The objective here is to look at the solution (V_i, Y_i) of (4.6) constructed in § 5 as a steady solution of the time-dependent problem (4.3) and to consider the stability of this solution to small perturbations of V_i and of Y_i. A study of the global stability of this solution is desirable but proves difficult due to the lack of a good comparison theorem for the adaptive methods. Instead we proceed by making an analysis of the local stability of the system obtained by linearizing (4.3) about the steady solution, in particular to find the dominant eigenvalues and eigenvectors of this linearization. We conclude from our calculations that the numerical self-similar solution is (neutrally) stable as $t \to \infty$. This behaviour reflects that of the self-similar solution of the underlying PDE.

Before making a detailed calculation we first exploit the action of the symmetry group to calculate three of the eigenvalues of the linearization of (4.3) about the self-similar solution. (Observe that as the differential and difference equations are invariant under the action of the same symmetry groups, then the same eigenvalues will be observed in both cases.) Suppose that $\boldsymbol{V} \equiv (V_i, \Lambda, Y_i)$ is a steady (self-similar) solution of (4.3). By the invariance of the underlying equation (3.11) to a translation in *time* we have that for all C

$$((t+C)^{1/3}t^{-1/3}V_i, (t+C)^{-1/3}t^{1/3}\Lambda, (t+C)^{-1/3}t^{1/3}Y_i)$$

is a solution of (4.3). As $t \to \infty$ this converges to $\boldsymbol{V}$. Similarly, by the invariance of (3.11) to translations in *space*, we have that for all D

$$(V_i, \Lambda, Y_i + Dt^{-1/3})$$

is a solution of (4.3) converging to $\boldsymbol{V}$. Finally, by invariance to *scaling* we have that for all ε

$$((1+\varepsilon)^2 V_i, (1+\varepsilon)\Lambda, (1+\varepsilon)Y_i)$$

is also a solution of (4.3). This does not converge to $\boldsymbol{V}$ but is close to it for all time showing that $\boldsymbol{V}$ is neutrally stable. Thus the group actions lead to infinitesimal perturbations to $\boldsymbol{V}$ of the form

$$(V_i, \Lambda, Y_i) + \frac{D}{t^{1/3}}(0, 0, \mathbf{1}) + \frac{C}{3t}(V_i, -\Lambda, -Y_i) + \varepsilon(2V_i, \Lambda, Y_i). \tag{6.1}$$

We now consider the full local stability of the steady-state discrete self-similar solution. To do this we denote the steady-state self-similar solution $\boldsymbol{V}$ by $(\bar{V}_i, \bar{\Lambda}, \bar{Y}_i)$ and seek infinitesimal time-dependent perturbations of the form

$$(V_i, \Lambda, Y_i) = (\bar{V}_i, \bar{\Lambda}, \bar{Y}_i) + \mathrm{e}^{\mu s}\boldsymbol{z}, \quad s = \log(t), \tag{6.2}$$

for appropriate eigenvalues μ and eigenvectors $\boldsymbol{z} \equiv (\varphi_i, \kappa, Z_i)$. From the above discussion we can already say that three values of μ and $\boldsymbol{z}$ are given by

$$(\mu, \boldsymbol{z}) = (0, (2\bar{V}_i, \bar{\Lambda}, \bar{Y}_i)), \quad (\mu, \boldsymbol{z}) = (-\tfrac{1}{3}, (0, 0, \mathbf{1})), \quad (\mu, \boldsymbol{z}) = (-1, (\bar{V}_i, -\bar{\Lambda}, -\bar{Y}_i)).$$

We now proceed to calculate further values of μ and $\boldsymbol{z}$. To perform this calculation it is useful to make a change of variables, which reduces the coupling between the mesh and the solution. If we set

$$W_i = \Lambda V_i \quad \text{and} \quad \chi = \Lambda^3, \tag{6.3}$$

then, from the conservation of I_N,

$$\sum_{i=0}^{N+1} W_i = \text{const.} \tag{6.4}$$

Recasting the equations (4.3) in terms of W_i, and expressing all derivatives with respect to the variable s, we have

$$\dot{W}_i = \tfrac{1}{3}W_i + \tfrac{1}{2}((W_{i+1} - W_{i-1})\dot{Y}_i + 2\dot{\Lambda}W_i) + \frac{1}{6\Lambda}(W_{i+1} - W_{i-1})Y_i + \tfrac{1}{2}((W_{i+1}^2 - 2W_i^2 + W_{i-1}^2)/\Lambda^3), \tag{6.5}$$

which can be expressed as a difference formula so that

$$\dot{W}_i = \alpha_i - \alpha_{i-1} + \beta_i - \beta_{i-1}, \tag{6.6}$$

where

$$\left.\begin{aligned} \alpha_i &= \frac{1}{2\Lambda}(W_{i+1}\dot{Y}_i + W_i\dot{Y}_{i+1}) + \frac{1}{6\Lambda}(W_{i+1}Y_i + W_iY_{i+1}),\\ \beta_i &= \frac{1}{2\Lambda^3}(W_{i+1}^2 - W_i^2). \end{aligned}\right\} \tag{6.7}$$

This is augmented by the boundary conditions

$$\tfrac{1}{3}Y_0 + \dot{Y}_0 = -W_1/\Lambda^2 \quad \text{and} \quad \tfrac{1}{3}Y_{N+1} + \dot{Y}_{N+1} = W_N/\Lambda^2. \tag{6.8}$$

Linear interpolation between Y_0 and Y_{N+1} gives

$$\alpha_i = \frac{1}{2\Lambda^3}\left[W_{i+1}\left(\frac{i}{N+1}W_N - \left(1 - \frac{i}{N+1}\right)W_1\right) + W_i\left(\frac{i+1}{N+1}W_N - \left(1 - \frac{i+1}{N+1}\right)W_1\right)\right], \tag{6.9}$$

and combining these results we have

$$\dot{W}_i = \frac{1}{2\chi}[\varphi_i - \varphi_{i-1}] \quad \text{and} \quad \dot{\chi} = -\chi + \frac{3}{N+1}(W_1 + W_N), \tag{6.10}$$

where

$$\varphi_i \equiv 2\chi(\alpha_i + \beta_i) \text{ depends only upon } W_i \text{ and not upon } \Lambda.$$

The formulation (6.10) of (4.3) separates the role played by the mesh and the solution on the mesh, and the local stability of these equations is more amenable to analysis. The system (6.10) has as a steady state the solution

$$\bar{W}_i = \bar{\Lambda}\bar{V}_i \quad \text{and} \quad \bar{\chi} = \bar{\Lambda}^3.$$

Suppose now that we linearize (6.10) about this steady state. This gives a linear system with Jacobian matrix J. A little calculation then shows that if A is the $N \times N$ matrix given by

$$A_{i,j} = \frac{\partial \varphi_i}{\partial W_j} - \frac{\partial \varphi_{i-1}}{\partial W_j} \tag{6.11}$$

evaluated at the steady state, then J is given by

$$J = \begin{bmatrix} & \frac{1}{2\bar{\chi}}A & & \mathbf{0} \\ \frac{3}{N+1} & 0\cdots 0 & \frac{3}{N+1} & -1 \end{bmatrix}. \tag{6.12}$$

Considering the small perturbation described in (6.2), suppose that J has an eigenvalue μ with corresponding (right) eigenvector $[e_i, 3\bar{\Lambda}^2\kappa]^{\mathrm{T}}$ such that $e_i = \bar{\Lambda}\varphi_i + \kappa\bar{V}_i$. Then

$$A\boldsymbol{e} = 2\bar{\chi}\mu\boldsymbol{e} \quad \text{and} \quad (e_1 + e_N)/(N+1) - \bar{\Lambda}^2\kappa = \mu\bar{\Lambda}^2\kappa.$$

Thus, either $\boldsymbol{e} = \mathbf{0}$, $\mu = -1$ or $\boldsymbol{e}$ is an eigenvector of A. This reduces the linear-stability problem to a study of the eigenvalues of A alone.

The following results follow immediately from the observations at the beginning of this section.

Lemma 6.1.

(i) *The matrix J has an eigenvalue of -1 with a right eigenvector $[\mathbf{0}, 1]^{\mathrm{T}}$.*

(ii) *The matrix A has a left null eigenvector $[1, 1, \ldots, 1]$ and a right null eigenvector $(W_1, W_2, \ldots, W_N)$.*

The matrix A inherits symmetries derived from the reflectional symmetry of the self-similar solution in which $\bar{V}_i = \bar{V}_{N+1-i}$. These imply that it has either even eigenvectors with $e_i = e_{N+1-i}$ or odd eigenvectors with $e_i = -e_{N+1-i}$. For the odd eigenvectors $e_1 + e_N = 0$, so that $\kappa = 0$ and the spacing Λ of the mesh does not change—although the position Y_i of the mesh does. The eigenvalues of A give all the values of μ stated in (6.2) apart from $\mu = -\frac{1}{3}$ and $\mu = -1$. Numerically calculated eigenvalues of A for $N = 8, 16, 32$ are given in table 1 together with an asymptotic value derived in formal proposition 6.2 (below). Observe that all of the calculated eigenvalues are real and negative, which strongly implies that the discrete self-similar solution is stable. In § 8 we give numerical evidence which supports the conjecture that the self-similar solution is globally asymptotically stable.

We do not yet have a rigorous proof of this result; however, strong evidence for it is given by the following.

Formal proposition 6.2. *Suppose that the values of μ are ordered such that $0 = \mu_0 > \mu_1 > \cdots$. Then in the limit of large N*

$$\mu_k \to -\tfrac{1}{6}k(k+1).$$

Note. For all N we have the three eigenvalues $\mu = 0, -\frac{1}{3}, -1$, and the numerical evidence strongly suggests that these are μ_0, μ_1, μ_2.

Formal derivation. It is simplest to show this for the case of an odd eigenvector. Here Λ does not change and we can put $Z_i = \theta$ for all i. A similar argument gives the more general case. Starting from

$$\dot{V}_i = \tfrac{1}{3}V_i + \frac{(V_{i+1} - V_{i-1})}{2\Lambda}\dot{Y}_i + \frac{(V_{i+1} - V_{i-1})}{6\Lambda}Y_i + \frac{(V_{i+1}^2 - 2V_i^2 + V_{i-1}^2)}{2\Lambda^2},$$

Table 1.

$N=8$	$N=16$	$N=32$	asymptotics
0.00000	0.00000	0.00000	0.00000
−1.74507	−1.90988	−1.97462	−2.00000
−2.60861	−3.00420	−3.23287	−3.33333
−3.69297	−4.17468	−4.69338	−5.00000
−5.25040	−5.57702	−6.31553	−7.00000
−7.26432	−7.36028	−8.08733	−9.33333
−9.66276	−9.58910	−10.12508	−12.00000
−12.41101	−12.23367	−12.53282	−15.00000
	−15.25429	−15.35969	−18.33333
	−18.62871	−18.59705	−22.00000
	−22.34468	−22.22073	−26.00000
	−26.39745	−26.21146	−30.33333
	−30.78515	−30.55471	−35.00000
	−35.50720	−35.24220	−40.00000
	−40.56338	−40.26866	−45.33333
	−45.95359	−45.63145	−51.00000
		−51.32913	−57.00000
		−57.36105	−63.33333
		−63.72690	−70.00000
		−70.42654	−77.00000
		−77.45990	−84.33333
		−84.82694	−92.00000
		−92.52763	−100.00000
		−100.56195	−108.33333
		−108.92987	−117.00000
		−117.63138	−126.00000
		−126.66646	−135.33333
		−136.03508	−145.00000
		−145.73724	−155.00000
		−155.77293	−165.33333
		−166.14213	−176.00000
		−176.84482	−187.00000

and substituting (6.2) gives (to leading order)

$$\mu\varphi_i = \tfrac{1}{3}\varphi_i + \mu\theta\frac{(\bar{V}_{i+1}-\bar{V}_{i-1})}{2\bar{\Lambda}} + \frac{(\varphi_{i+1}-\varphi_{i-1})}{6\bar{\Lambda}}Y_i + \frac{(\bar{V}_{i+1}-\bar{V}_{i-1})}{6\bar{\Lambda}}\theta + \frac{\bar{V}_{i+1}\varphi_{i+1}-2\bar{V}_i\varphi_i+\bar{V}_{i-1}\varphi_{i-1}}{\bar{\Lambda}^2}, \quad (6.13)$$

with boundary conditions

$$\tfrac{1}{3}\theta+\mu\theta = -\varphi_1/\bar{\Lambda}, \quad \tfrac{1}{3}\theta+\mu\theta = \varphi_N/\bar{\Lambda}, \quad \varphi_0=\varphi_{N+1}=0. \quad (6.14)$$

Now consider the limit of $N\to\infty$. In this case $\bar{\Lambda}\to 0$, and (as in § 5) we may set $\varphi_i=\varphi(Y_i)$. In the limit, (6.13) becomes

$$\mu\varphi = \tfrac{1}{3}\varphi + \tfrac{1}{3}y\varphi_y + (v\varphi)_{yy} + \theta(\tfrac{1}{3}+\mu)v_y,$$

with boundary condition

$$\theta(\tfrac{1}{3}+\mu) = -\varphi_y(-L) = -\varphi_y(L).$$

Now substitute the limiting function $v(y) = a - \frac{1}{6}y^2$ to give

$$\mu\varphi = ((a - \tfrac{1}{6}y^2)\varphi_y)_y - \tfrac{1}{3}\theta y(\tfrac{1}{3} + \mu).$$

This is a perturbation of Legendre's equation. If k is *odd* and $P_k(z)$ is the kth Legendre polynomial defined on the interval $[-1, 1]$ normalized such that $P_k(1) = 1$, then a simple calculation gives

$$\mu = -\tfrac{1}{6}k(k+1), \qquad \varphi(y) = \tfrac{1}{3}\theta L(P_k(y/L) - y/L).$$

This is the formal result required. ■

Inspection of the tabulated values shows good agreement with the asymptotic values for small values of k.

7. Convergence

Based upon the results of the previous section we now make some statements about the convergence of the discrete solution of the original discretization of the PME to the true solution of the PME. Suppose that we start with an initial function $u(x, 0)$ with integral $I = 1$ and centre of mass $\bar{X} = 0$ such that the support of $u(x, 0)$ is $s_-(0), s_+(0)$. Now discretize $u(x, 0)$ to give $U_i(0)$ by sampling at equally spaced points X_i, and set $X_0(0) = s_-(0), X_{N+1}(0) = s_+(0)$. By standard results on quadrature we have values A, B such that

$$I_N = 1 + \frac{A}{(N+1)^2} + \mathcal{O}(1/N^4), \quad \bar{X}_N = \frac{B}{(N+1)^2} + \mathcal{O}(1/N^4).$$

Following our stability calculations we can now presume that U_i and X_i when rescaled tend toward the discrete self-similar solution so that

$$t^{1/3}U_i = V_i + \mathcal{O}(1/t) \quad \text{and} \quad t^{-1/3}X_i = Y_i + \mathcal{O}(B/(N+1)^2t^{1/3}) + \mathcal{O}(1/t).$$

We also have that

$$t^{1/3}u(X_i, t) = v(t^{-1/3}X_i) + \mathcal{O}(1/t) = v(Y_i) + \mathcal{O}(B/(N+1)^2t^{1/3}) + \mathcal{O}(1/t).$$

Combining these results gives the convergence result

$$t^{1/3}(U_i(t) - u(X_i, t)) = V_i - v(Y_i) + \mathcal{O}(B/(N+1)^2t^{1/3}) + \mathcal{O}(1/t).$$

For large t the dominant error contribution thus comes from the term $E_i \equiv V_i - v(Y_i)$. This we can estimate from the results of § 5. To do this we must compare like functions. Observe that if $\Lambda = t^{-1/3}H$, then to leading orders

$$\Lambda \sum_{i=0}^{N+1} V_i = I_N = 1 + \frac{A}{(N+1)^2}.$$

To apply the analysis of § 5 we set

$$\hat{V}_i = I_N^{-2/3}V_i, \quad \hat{Y}_i = I_N^{-1/3}Y_i \quad \text{and} \quad \hat{\Lambda} = I_N^{-1/3}\Lambda.$$

Then $(\hat{V}_i, \hat{Y}_i)$ satisfies the equations for the discrete self-similar solution and

$$\hat{\Lambda} \sum_{i=0}^{N+1} \hat{V}_i = 1.$$

Now, from § 5, $\hat{V}_i = v_i + w_i$ with v_i, y_i and w_i given by (5.1), (5.2) and (5.14). Furthermore,

$$Y_i = I_N^{1/3}\hat{Y}_i = y_i(1+\theta)I_N^{1/3} = y_i\left(1+\theta+\frac{1}{3}\frac{A}{(N+1)^2}\right),$$

so that

$$\begin{aligned} v(Y_i) &= v\left(y_i\left(1+\theta+\frac{1}{3}\frac{A}{(N+1)^2}\right)\right) \\ &= v_i + y_i\left(\theta+\frac{1}{3}\frac{A}{(N+1)^2}\right)v'(y_i) \\ &= v_i - \tfrac{1}{3}\theta y_i^2 - \frac{1}{9}\frac{Ay_i^2}{(N+1)^2}. \end{aligned}$$

Thus,

$$\hat{V}_i - v(Y_i) = w_i + \tfrac{1}{3}\theta y_i^2 + \frac{1}{9}\frac{Ay_i^2}{(N+1)^2}.$$

But

$$\hat{V}_i = \left(1-\frac{2}{3}\frac{A}{(N+1)^2}\right)V_i = V_i - \frac{2}{3}\frac{A}{(N+1)^2}V_i,$$

so to leading order

$$\begin{aligned} V_i - v(Y_i) &= w_i + \tfrac{1}{3}\theta y_i^2 + \frac{1}{9}\frac{Ay_i^2}{(N+1)^2} + \frac{2}{3}\frac{A}{(N+1)^2}(a - \tfrac{1}{6}y_i^2) \\ &= w_i + \tfrac{1}{3}\theta y_i^2 + \frac{2}{3}\frac{Aa}{(N+1)^2}. \end{aligned}$$

Using the outer expression (5.14) for w_i, valid away from the interface, we then have

$$E_i = \frac{1}{(N+1)^2}(\kappa + 2a\log(a - \tfrac{1}{6}y_i^2) + \tfrac{2}{3}Aa). \tag{7.1}$$

The function E_i has a maximum at $y = 0$ where it equals

$$E_{\mathrm{mid}} \equiv \frac{1}{(N+1)^2}(\alpha + 2a\log(a) + \tfrac{2}{3}Aa).$$

As $|y| \to L$, E_i is negative and increases in absolute value, so that the largest error occurs at the interface itself. At this point we have $w_i = 0$ and $y_i^2 = L^2 = 6a$ so that $E_i \equiv E_{\max}$, where

$$E_{\max} = 2\theta a + \frac{2}{3}\frac{Aa}{(N+1)^2} = \frac{2a}{(N+1)^2}(\delta - \log(N+1) + \tfrac{1}{3}A). \tag{7.2}$$

The two expressions (7.1), (7.2) thus give the forms of the scaled error at the midpoint and at the interface. Observe that the dominant error at the interface is asymptotically proportional to $\log(N+1)/(N+1)^2$ and is independent of the initial conditions. In contrast, the error at the midpoint is asymptotically proportional to $1/(N+1)^2$ and depends strongly upon the initial conditions.

figure 2

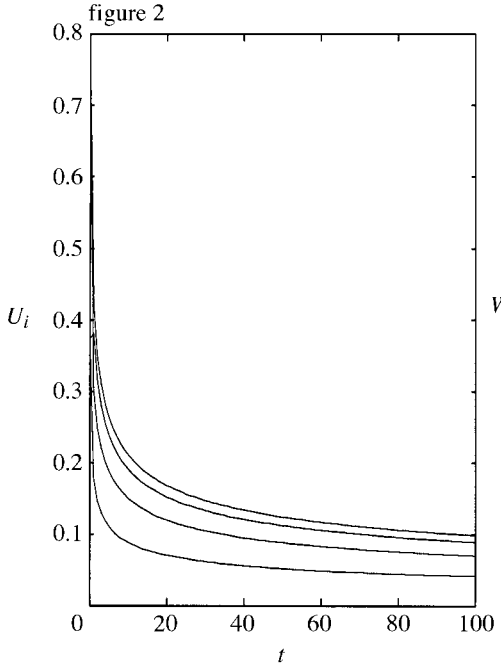

figure 3

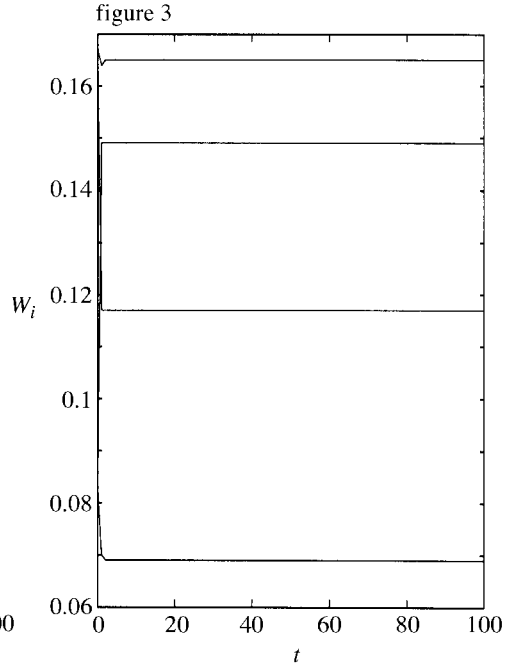

Figure 2. Symmetric behaviour of U_i.

Figure 3. Symmetric behaviour of W_i.

We can also estimate the mean-square error of the calculation. Suppose that we define the discrete L_2 error by

$$\|U_i(t) - u(X_i, t)\|_2^2 = \sum_{i=0}^{N+1} H(U_i - u(X_i))^2. \tag{7.3}$$

Then a simple calculation shows that to leading order we can estimate this by

$$t^{1/6}\|U_i(t) - u(X_i, t)\|_2 = \sqrt{\int_{-L}^{L} E^2 \,\mathrm{d}y}. \tag{7.4}$$

Using the expression for E, all quadratures can be evaluated to give

$$t^{1/6}\|U_i(t) - u(X_i, t)\|_2 \equiv E_{L_2} = \frac{1}{(N+1)^2}\sqrt{2.238\,302 + 0.605\,687A + 0.302\,828A^2}. \tag{7.5}$$

Observe that the mean-square error scales as $1/(N+1)^2$. In this it differs from the mean-square error of the self-similar solution computed in § 5, which scales as $\log(N+1)/(N+1)^2$.

8. Numerical results

In this section we consider three numerical calculations. Firstly, we look at the convergence of the discrete self-similar solution to the true self-similar solution. Secondly, we look at the stability of the discrete self-similar solution. Finally, we look at the convergence of the numerical solution to the PDE.

figure 4

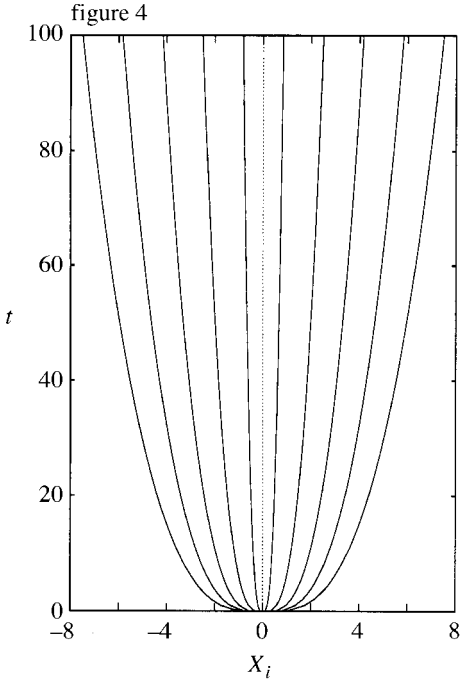

figure 5

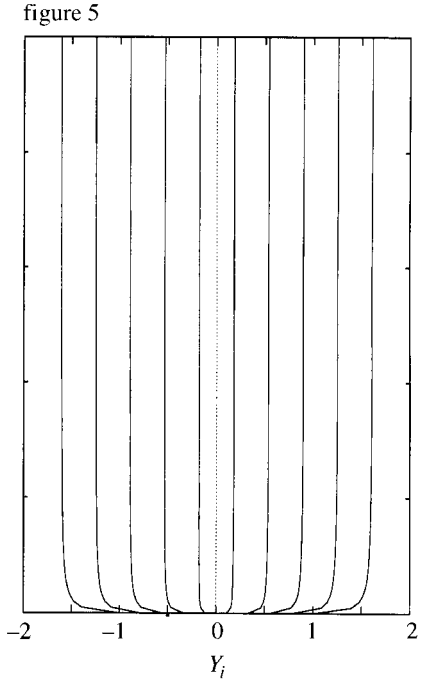

Figure 4. Symmetric behaviour of X_i.

Figure 5. Symmetric behaviour of Y_i.

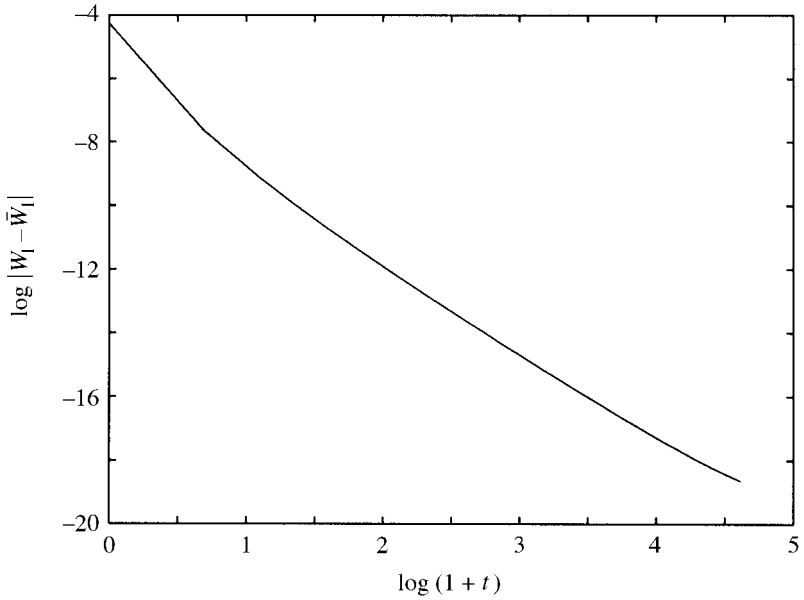

Figure 6. Convergence of the scaled solution.

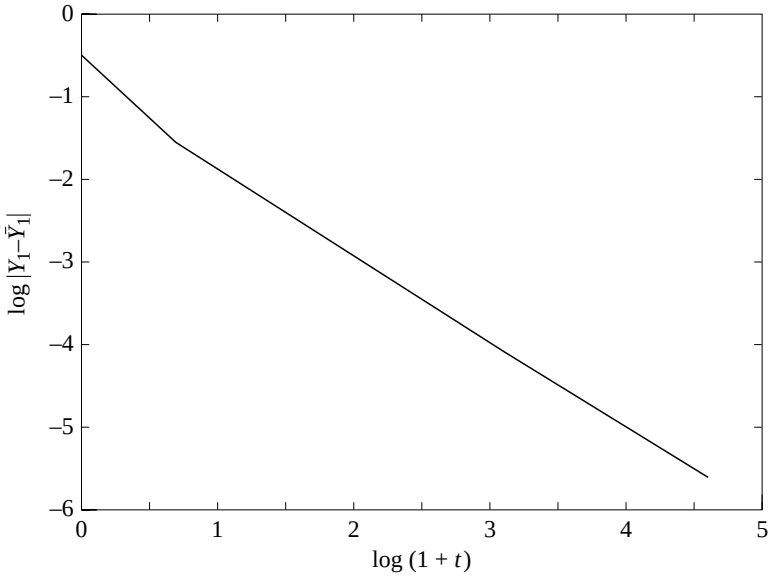

Figure 7. Convergence of the scaled mesh.

figure 8

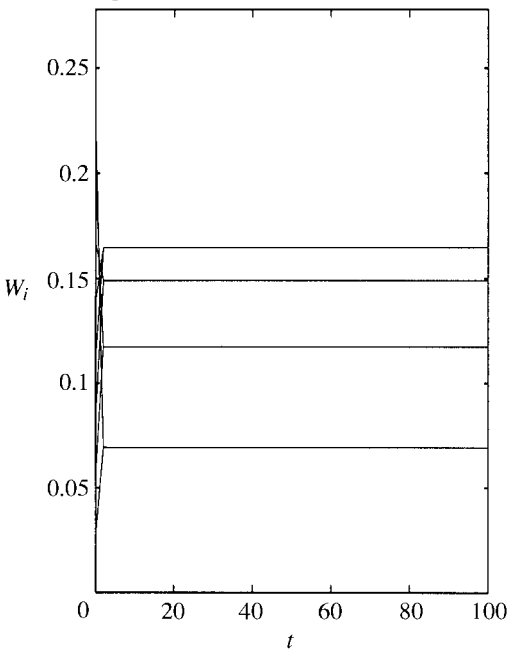

figure 9

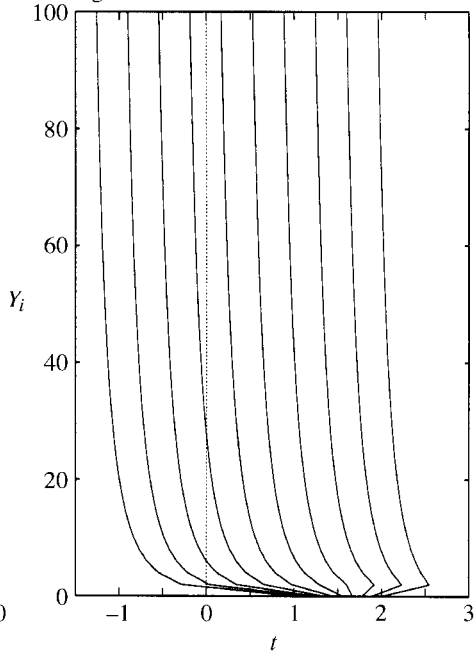

Figure 8. Asymmetric behaviour of W_i.

Figure 9. Asymmetric behaviour of Y_i.

figure 10

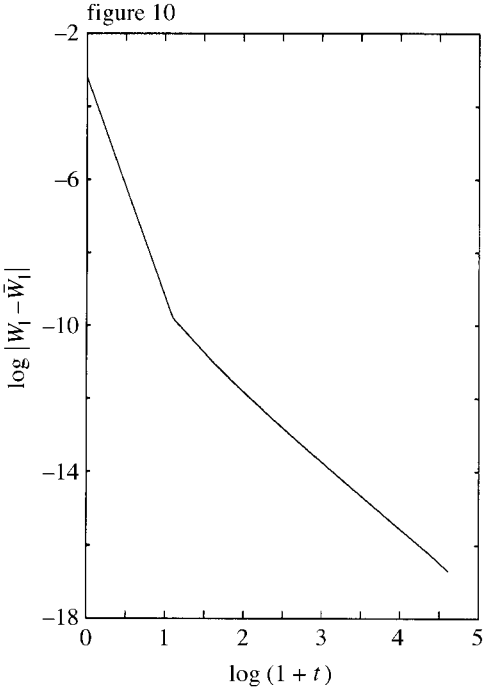

figure 11

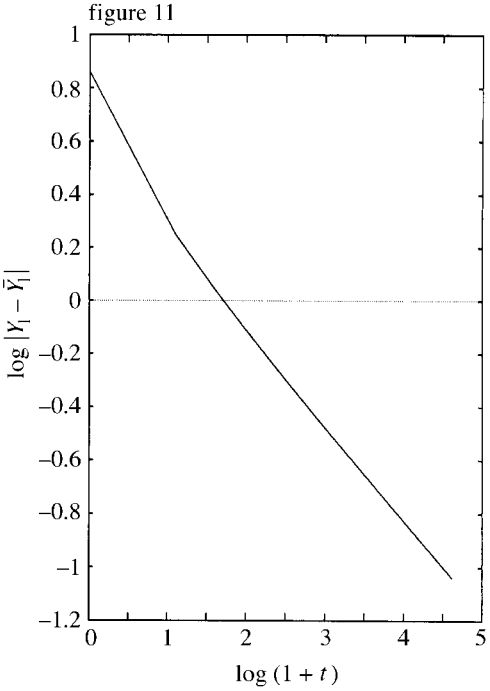

Figure 10. Convergence of asymmetric W_i.

Figure 11. Convergence of asymmetric Y_1.

(a) *Convergence of the self-similar solution*

We first consider the convergence of the discrete self-similar solution V_i to the point values v_i of the true self-similar solution. To do this we take $N = 31, 63, 127$ and find the solution of the nonlinear system (4.11) using the Powell hybrid solver SNSQE. We then calculate $S_a = V_{(N+1)/2} - v_{(N+1)/2}$ and $S_b = \max_i |V_i - v_i|$ and compare these values with the asymptotic values S_{mid} and $|S_{\max}|$ given by (5.3) and (5.22), respectively. The resulting values are as follows:

N	S_a	S_{mid}	S_b	$\lvert S_{\max}\rvert$
31	0.000837	0.000840	0.001706	0.001718
63	0.000210	0.000210	0.000533	0.000539
127	0.000053	0.000053	0.000163	0.000164

.

The agreement between the asymptotic and numerical estimates is very good indeed, giving us great confidence in the validity of the asymptotic approach.

(b) *Stability*

We now give results of some computations of the system (4.3) for fixed N letting $t \to \infty$. For convenience we keep $N = 8$ fixed throughout. The ODEs arising were solved using DASSL with a solution tolerance of 10^{-10}. In all computations the self-similar solution was found to be globally stable.

Example 8.1. For our first computation we take as initial values

$$\{U_i\} = \tfrac{9}{24}\{1,2,1,2,2,1,2,1\} \quad \text{and} \quad \{X_0, X_9\} = \{-1,1\}.$$

These data are symmetric, and we have $I_8 = 1$ and $\bar{X} = 0$. In figures 2 and 3 we plot the values of U_i and $W_i = HU_i$ as functions of t for $0 \leqslant t \leqslant 100$, and in figures 4 and 5 the mesh and scaled mesh X_i and $Y_i = (t+1)^{-1/3}X_i$. Here we scale with $t+1$ rather than with t to avoid problems when $t = 0$. Observe that W_i very rapidly tends towards a constant value, whereas Y_i takes rather longer to converge. In figures 6 and 7 we plot $\log|W_1 - \bar{W}_1|$ and $\log|Y_1 - \bar{Y}_1|$, respectively, as functions of $\log(t+1)$, where $\bar{W}$ and $\bar{Y}$ now refer to the steady self-similar solution. Observe that each graph is close to linear, implying that the linear-stability results of § 6 are appropriate. The gradient of the first graph is very close to -1. This is as predicted and is due to the arbitrary nature of the choice of time origin. In contrast, the second graph has a gradient of -2.68 corresponding to the eigenvalue μ_4 with a corresponding symmetric eigenvector.

Example 8.2. For our second computation we take the asymmetric initial data

$$\{U_i\} = \tfrac{1}{4}\{1,2,3,4,5,6,7,8\} \quad \text{and} \quad \{X_0, X_9\} = \{1,2\},$$

for which again $I_8 = 1$ but $\bar{X} \neq 0$. The values of W_i and Y_i are plotted in figures 8 and 9 and the convergence to the steady state examined in figures 10 and 11, which correspond directly to figures 6 and 7. Observe in this case that Y_i converges much more slowly to the steady state. Indeed the gradient of the curve in figure 10 is proportional to $-1/3$ due to the arbitrary choice of the origin for the spatial coordinate. The rate of convergence of W_i is also slower, with gradient -1.74507, corresponding to the eigenvalue μ_3 with an odd eigenvector.

(*c*) *Convergence*

We now provide some numerical support for the results of § 7. To do this we consider two examples.

Example 8.3. For our first example we take as initial data the exact self-similar solution $u(x,0) = (a - \frac{1}{6}x^2)$ with unit first integral and interpolate to give U_i. A straightforward calculation then gives the quadrature error as $I_N = 1 - 1/(N+1)^2$ so that $A = -1$. We then calculate the values of

$$E_a \equiv (1+t)^{1/3}(U_{N2} - u(0,t)),$$
$$E_b \equiv (1+t)^{1/3} \max|U_i(t) - u(X_i,t)|,$$
$$E_c \equiv (1+t)^{1/6}\|U_i(t) - u(X_i(t))\|_2,$$

where $N2 = \frac{1}{2}(N+1)$ and $u(x,t)$ can be calculated exactly. These values can be compared directly with E_{mid}, $|E_{\max}|$ and E_{L_2} given in (7.1), (7.2) and (7.3). As U_i is close to the initial values of the discrete self-similar solution, convergence in time to the scaled error occurs quickly, and we compare scaled errors at $t = 100$ for $N = 31, 63, 127$. The results are given in the following and show very good agreement between numerical and asymptotic results:

N	E_a	E_{mid}	E_b	$\lvert E_{\max}\rvert$	E_c	E_{L_2}
31	0.000533	0.000545	0.003022	0.003073	0.001334	0.001461
63	0.000134	0.000136	0.000910	0.000922	0.000335	0.000365
127	0.000034	0.000034	0.000266	0.000269	0.000084	0.000091

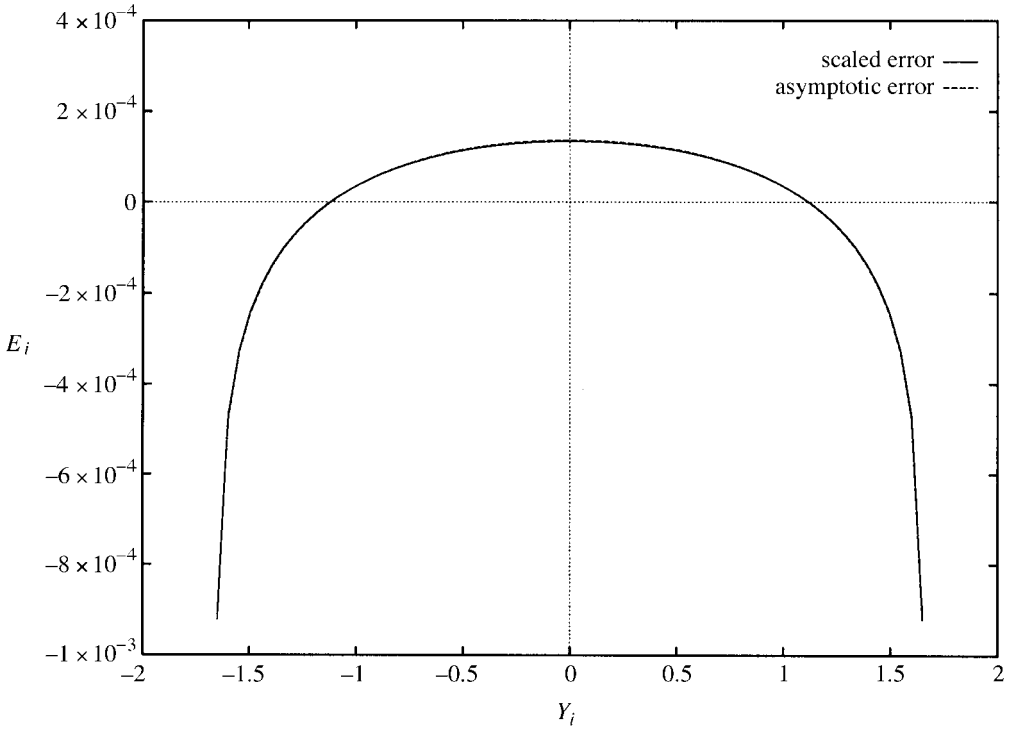

Figure 12. A comparison of the computed scaled error and the asymptotic error.

Observe that E_b is much greater than E_a and E_c.

We can also compare the function E_i as estimated asymptotically in (7.1) with the values of $(t+1)^{1/3}(U_i - u(X_i, t))$. This is given in figure 12. Again the agreement between asymptotics and numerical results is very good.

Example 8.4. In this example we take as initial data $U_i = 1/N$. For these data we have $I_N = 1$ so that $A = 0$. The form of the resulting solution $u(x,t)$ is not known explicitly in this case, though we do know that it converges to the self-similar solution. Thus, for long times we can compare U_i with the self-similar solution and calculate E_a and E_b using this. In this case we expect E_1 and E_2 to converge to E_{mid} and $|E_{\max}|$ as before—though the convergence will take longer. In practice, we do not see convergence until $t > 1000$. The results are then very similar to those given above.

References

Barenblatt, G. I. 1996 Scaling, self-similarity and intermediate asymptotics. *Cambridge texts in applied mathematics*, vol. 14. Cambridge University Press.

Bluman, G. & Cole, J. 1974 *Similarity methods for differential equations*. New York: Springer.

Budd, C. J. & Collins, G. J. 1998 Symmetry based numerical methods for partial differential equations. In *Numerical analysis 1997* (ed. D. Griffiths, D. Higham & G. Watson), *Pitman Research Notes in Mathematics Series*, vol. 380, pp. 16–36, London: Longman.

Budd, C. J., Huang, W. & Russell, R. D. 1996*a* Moving mesh methods for problems with blow-up. *SIAM J. Sci. Comp.* **17**, 305–327.

Budd, C. J., Chen, J., Huang, W. & Russell, R. D. 1996*b* Moving mesh methods with applications to blow-up problems for PDEs. In *Numerical analysis 1995* (ed. D. Griffiths & G. Watson), pp. 1–18. *Pitman Research Notes in Mathematics Series*, vol. 344. London: Longman.

Dorodnitsyn, V. 1993 Finite difference methods entirely inheriting the symmetry of the original equations. In *Modern group analysis: advanced analytical and computational methods in mathematical physics* (ed. N. Ibragimov), pp. 191–201. Kluwer Academic.

Dresner, L. 1983 Similarity solutions of nonlinear partial differential equations. *Pitman Research Notes in Mathematics Series*, vol. 88. London: Longman.

Huang, W., Ren, Y. & Russell, R. D. 1994 Moving mesh methods based on moving mesh partial differential equations. *J. Comp. Phys.* **112**, 279–290.

Kamenomostskaya, S. 1973 The asymptotic behaviour of the solution of the filtration equation. *Israel J. Math.* **14**, 76–87.

Murray, J. D. 1989 *Mathematical biology*. New York: Springer.

Olver, P. 1986 Applications of Lie groups to differential equations. New York: Springer.

Petzold, L. R. 1982 A description of DASSL: a differential/algebraic system solver. Report SAND82-8637, Sandia National Laboratories.

Ralston, J. 1984 A Lyapunov functional for the evolution of solutions to the porous medium equation to self-similarity. II. *J. Math. Phys.* **25**, 3124–3127.

Vazquez, J. L. 1992 An introduction to the mathematical theory of the porous medium equation. In *Shape optimisation and free boundaries* (ed. M. Delfour), pp. 347–389. Dordrecht: Kluwer.

PHILOSOPHICAL TRANSACTIONS OF THE ROYAL SOCIETY A MATHEMATICAL, PHYSICAL & ENGINEERING SCIENCES

PHILOSOPHICAL TRANSACTIONS OF THE ROYAL SOCIETY A MATHEMATICAL, PHYSICAL & ENGINEERING SCIENCES